Application of the ground cooling system for rural houses air conditioning in northeastern China

Moon Ki Jang

(*College of Information & Electric Engineering, Shenyang Agricultural University, Shenyang 110161, China*)

Abstract: This study developed an appropriate ground cooling system that can be used for indoor cooling during summers in rural houses in northeastern China.   To apply this system, a traditional rural house was selected and a heat exchanger was designed (PE pipe, 32 m in length), manufactured, and installed according to the cooling load (2206 kJ/h) of one room of the experimental house.   According to the experiment, the temperature of Room 1 equipped with the cooling system was 3 ℃ lower than that of Room 2 without the ground cooling system during the same time period.   The temperature reduction effect of this system was confirmed through this study.   When the ground cooling system was used in rural houses in Northeast China, it was found that a burial depth of 1.5-2.0 m for the ground heat exchanger is appropriate for considering workability and frost line.   The use of the ground cooling system for indoor cooling during summers for rural houses in the northeastern region of China would reduce not only environmental pollution and the use of fossil fuels but also ease farmers off a certain amount of financial burden.
Keywords: ground cooling system, ground heat exchanger, air conditioning system, rural houses
DOI: 10.25165/j.ijabe.20221502.6223

1   Introduction

Recently, in many countries globally, alternative energy resources are being developed to secure future energy sources and ensure environmental protection[1,2].   Additionally, to actively adapt to changes resulting from climate change conventions, new and renewable energy sources such as solar, wind, and geothermal energy are being developed[3].

Of these sources, geothermal energy, which is a clean source of energy with high application potential not only for agriculture but also in other fields, remains constant throughout the year[4,5].   Underground heat can be directly used.   However, the generally used method is to conduct a convenient heat transfer through a heat pump system.   This is beneficial for intensifying the ground heat so that the ground can be used as a heat source for heating and as a heat sink for cooling purposes[6,7].

A ground cooling system can be categorized into two general types, depending on the heat source being used.   The closed-loop type involves a heat exchanger installed underground, where cooling is circulated through an internal pipe.   On the other hand, the open-loop type uses ground, underground water, or external air directly.   Regarding the Earth's surface, the underground temperature hardly changes below the frost line throughout the year[8,9].   The annual average underground temperature below the frost line ranges between 10 ℃ and 18 ℃.   Thus, it has a high potential for use as a cold heat source for ground cooling systems, besides being highly stable.   In fact, many studies on such ground cooling systems are being conducted globally[10,12].

In Japan, a specific burial depth of 50 cm and an interval location of 50-60 cm of pipes for harnessing underground heat have been suggested[13].   Puri[14] studied the appropriate number of hours required for recharging using the finite-element method and interpreted a two-dimensional stationary-state equation using the boundary-element method.   He reported that the stationary-state analysis was within a reasonable error range considering long-term performance.   Gao et al.[15] presented a technical route for ground heat exchangers to help realize zero energy buildings, which provides a promising solution to improve energy efficiency of buildings through an experiment in China.   Lekhal et al.[16] studied thermal performance of a residential house equipped with a direct solar floor and an earth-air heat exchanger.   Javadi et al.[17] analyzed the performance of ground heat exchangers with different configurations.   Kim et al.[18] studied the heat transfer characteristics of the heat exchangers according to pipe laying intervals under the ground by the numerical analysis in South Korea.   He emphasized that the installation interval of heat exchanger is very important.   This is because the shorter the burial interval of the pipes, the greater the heat loss through the ground surface, thereby decreasing the efficiency of the underground heat exchange.   Furthermore, Park et al.[19-21] reviewed the heat-exchange amount, heat-exchange efficiency, coefficient of performance, and appropriate length of buried pipes to analyze the effects of atmospheric air on a ground heat exchanger.   Because most of these studies were largely theoretical or the conditions were very different everywhere, it is not enough or suitable to use the above results for air conditioning of rural houses in northeast China[22-24].

This study aims to develop a ground cooling system so that a geothermal energy source can be used for indoor cooling in rural houses in northeast China during summers and to propose various conditions for a ground cooling system.

2   Ground cooling system

2.1   Thermal energy transport

The underground temperature on the Earth's surface hardly changes throughout the year under a certain depth below the frost

line of any location.　The annual average ground-temperature range below the frost line is 10℃-18℃.

Through porous media, heat energy is transferred by conduction, convection, and radiation.　In this study, the considered means of transferring heat energy included forced convection (fluid flow) and heat conduction using Darcy's law[25]. The equation can be expressed three-dimensionally as follows:

$$H_x = -K_{ex}\left(\frac{\partial T}{\partial x}\right) + n\rho_w C_w T V_x \tag{1}$$

$$H_y = -K_{ey}\left(\frac{\partial T}{\partial y}\right) + n\rho_w C_w T V_y \tag{2}$$

$$H_z = -K_{ez}\left(\frac{\partial T}{\partial z}\right) + n\rho_w C_w T_z \tag{3}$$

where, H is the heat flux, kJ; K_e is the effective thermal conductivity, kJ/(h·m·℃); T is the temperature, ℃; $n\rho_w C_w$ is the total heat amount of underground water (fluid) stored per unit volume of the underground medium; V is the velocity vector of the underground water; x, y, and z refer to the three-dimensional directions.

In the thermal conductive-convective equation defined above, the following assumptions can be made: underground water flow was in a state of equilibrium (i.e., steadily flowing), underground water current speed was 0, and the underground temperature was in a normal state.　The amount of underground heat transfer can be expressed as[26]:

$$K_e \nabla^2 T - n\rho_w C_w V \cdot \nabla T = 0 \tag{4}$$

where, H is the heat flux, kJ; K_e is the effective thermal conductivity, kJ/(h·m·℃); T is the temperature, ℃; $n\rho_w C_w$ is the total heat amount of underground water (fluid) stored per unit volume of the underground medium; x, y, and z refer to the three-dimensional directions; V is the velocity vector of the underground water.

2.2　Cooling load

Cooling load refers to the amount of heat that needs to be removed in correspondence with the indoor heat gain to maintain a constant indoor temperature and humidity.　The total cooling load (Q_c) of the experimental building was calculated by the following equations[27-30].

$$Q_c = (Q_s + Q_c + Q_i + Q_{oa}) + Q_w \tag{5}$$

where, Q_s is the amount of solar heat acquired through the window, kJ/h; Q_c is the amount of heat obtained through the surface of the building, kJ/h; Q_i is the amount of sensible heat acquired by the infiltrated wind to the building, kJ/h; Q_{oa} is the amount of heat generated by the human body indoors, kJ/h; Q_w is the amount of acquired latent heat, kJ/h.

The amount of solar heat acquired through the window (Q_s) was applied according to various types (windows, entrances, etc.), the amount of heat conduction obtained through the surface of the building (Q_c) was calculated according to the following equation:

$$Q_c = (UA)(DETD) \tag{6}$$

where, U is the total heat transfer coefficient, kJ/(h·m²·℃); A is the total surface area, m²; $DETD$ is the design equivalent temperature difference, ℃.

The amount of sensible heat acquisition (Q_i) by the infiltrated wind was calculated according to the following equation:

$$Q_i = 0.018V(T_o - T_i) \tag{7}$$

where, V is the air change rate, times/h; T_o is the outdoor air temperature, ℃; T_i is the designed indoor temperature, ℃.

Also, the amount of latent heat acquisition (Q_w) to increase the humidity of the infiltrated wind to the level of the room was calculated according to the following equation:

$$Q_w = 79.5V_i(W_o - W_i) \tag{8}$$

where, V_i is the air permeability, m³/h; W_i is the relative humidity of indoor air, %; W_o is the relative humidity of outdoor air, %.

3　Experimental materials and methods

3.1　Experimental outline

This experiment was conducted for about a month, starting from August 16th, 2018, to September 15th, 2018, in Shejia village (testing place), Liaozhong-xian, Shenyang City, Liaoning Province, China.　The latitude, longitude, and altitude of the sites were 41°41′14″, 113°44′30″, and 82 m above sea level, respectively. Figures 1 and 2 show the cross-sectional view of the cooling system, which used a ground heat exchanger, and the floor plan of the ground heat exchanger installation, respectively.

As shown in the figures, the isolated loss cooling system is a type of ground cooling system that can decrease the indoor temperature by allowing outdoor air in the northern part of the building to go through the ground heat exchanger, thus guiding more cool air to the inside, using a fan, while ventilating the indoor air in the southern direction[31].
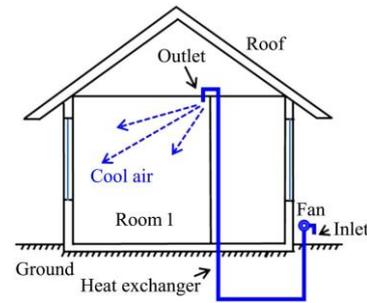
Figure 1　Cross-sectional view of ground cooling system
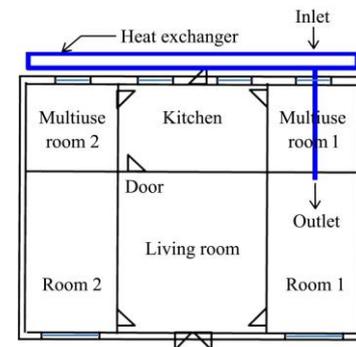
Figure 2　Floor plan of the ground heat-exchanger installation

3.2　Experiment material

The soil at the experimental site comprised sand (77%), silt (18%), and clay (5%) and had a water uptake rate of 39%.　The soil's heat conductivity was 0.654 W/(m·℃).　The polyethylene (PE) pipe used in the heat exchanger had an external diameter of 60.33 mm, an internal diameter of 52.5 mm, thermal resistance of 0.066 (m·h·℃)/kJ, and allowable stress of 0.80 MPa.

The total length of the ground heat exchanger was 32 m. Figures 3 and 4 and Table 1 show the values for the wall, roof structure, and materials of the experimental house, respectively. The house was a one-story building, facing south, as shown in Figure 5, and its residents included two adults and one child. Figure 6 shows the locations of the temperature sensors.
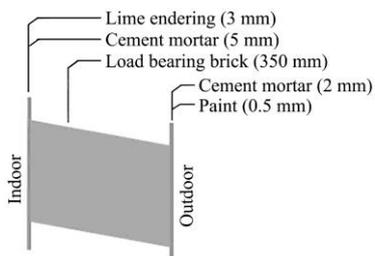
Figure 3   Structures of outdoor wall
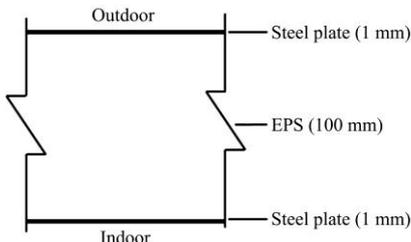
Figure 4   Structures of living roof

Table 1   Properties of building materials

Material No.	Material name	Density /kg m^{-3}	Thermal conductivity /W m^{-1}·$℃^{-1}$	Thermal capacity /J kg^{-1}·$℃^{-1}$
1	Expanded PS	25	0.035	1380
2	Load-bearing brick	900	0.036	936
3	Lime rendering	1800	0.87	-
4	Cement mortar	2000	1.4	800
5	Paint	-	-	-
6	Steel plate	7913	15.6	456

Figure 5   Typical rural house
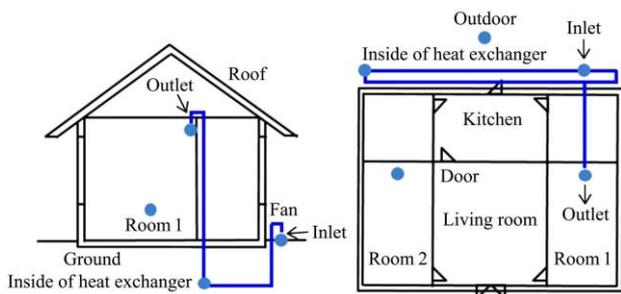
Figure 6   Locations of temperature sensors

3.3   Experimental method

To develop an appropriate ground cooling system that can utilize the cool underground temperature for rural houses in northeastern China during summers, a typical house was selected and its cooling load was calculated. A PE pipe heat exchanger suitable for the cooling load of the house was then manufactured. The total length (32 m) of the heat exchanger was determined according to the workability and heat-exchange amount, and then the exchanger was buried underground (depth of 1.5 m), as shown in Figures 7 and 8.

To calculate the heat-exchange amount and heat-exchange efficiency, and to analyze the indoor temperature changes, the

internal heat exchanger and changes in humidity were installed at nine locations, as shown in Figure 6. Using automatic data acquisition equipment, temperature and humidity data were measured, as shown in Figure 9.
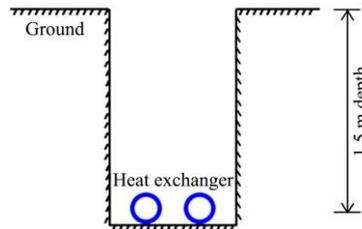
Figure 7   Underground cross-sectional view

Figure 8   Underground installation of PE pipe

Figure 9   Automatic data acquisition equipment and sensor installation

4   Experimental results and analysis

4.1   Temperature change per ground depth

Figure 10 shows the changes in monthly average ground temperatures for a year according to the ground depth from the surface at the experiment site. The lowest temperatures at depths of 1 m and 2 m were 11.9 ℃ and 11.7 ℃, respectively, both of which occurred at the end of March due to a time lag. The highest temperatures were 18.3 ℃ and 17.7 ℃, recorded at the beginning of October. At a depth of 5 m, the lowest temperature was recorded as 10.5 ℃ during March and the highest temperature was recorded as 16.2 ℃ at the end of November.
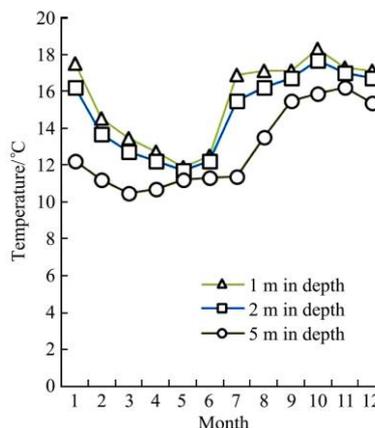
Figure 10   Ground temperature changes

The recorded differences in monthly average ground temperatures for a year between depths of 1 m and 5 m was 2.6℃. The highest and lowest temperatures at depths of 1 m and 2 m occurred simultaneously, whereas at the 5 m depth, the highest temperature was recorded one month later and the lowest temperature was recorded 2 months earlier.   Due to the time lag, the temperature difference between the underground depths of 1 m and 5 m was not very significant.   In addition, even in the hottest month of August, the temperatures at depths of 1 m and 2 m were both within 0.9℃, without a significant difference in temperatures.

4.2   Change in temperature and relative humidity

Figure 11 shows the daily-hourly average temperature change of each point according to time.   R1T is the Room 1 temperature of the room where the cooling system was installed, whereas R2T shows the Room 2 temperature of the room without any cooling system, which was used as a control specimen for R1T.   ITGHE indicates the interior temperature of the ground heat exchanger, whereas OAT shows the outdoor-air temperature.

As shown in Figure 11, the times for which the highest temperatures were recorded according to the daily time changes were between 1:00-2:00 pm outside; between 4:00-5:00 pm in Room 1; at 3:00 pm in Room 2, which was 1-2 h earlier than that in Room 1; and between 4:00-5:00 pm in the interior of the ground heat exchanger, which was the same as that in Room 1.
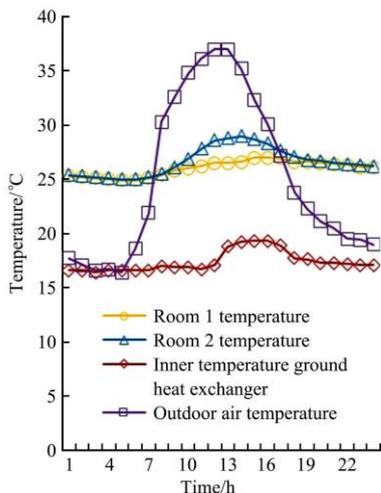
Figure 11   Temperature change of various points

In Rooms 1 and 2, an indoor temperature exceeding 26℃ continued for 15 h and 16 h, respectively.   An indoor temperature exceeding 28℃ continued for 0 h for Room 1 h and 5 h for Room 2. The highest, lowest, and average temperatures inside the heat exchanger were 19.3℃, 16.4℃, and 17.4℃, respectively, and temperature difference between the interior and exterior of the ground heat exchanger was 7.7℃.

The temperature difference between the highest and lowest temperatures of the ground heat exchanger inside was approximately 3℃, and was very small and stable compared to the outdoor temperature and the temperature in both rooms.   Because of the operation of the cooling system, the temperature difference between the two rooms was maintained for 12 h (from 9:00 am to 9:00 pm) during a 24 h period, whereas the indoor temperature in Room 1 was 0.9℃ lower than that in Room 2, as shown in Figure 12.

Figure 13 shows the relative indoor humidity change.   Here, R1RH shows the relative humidity of Room 1 equipped with a ground cooling system, whereas R2RH shows the relative humidity

of Room 2 without any cooling system.   As shown in Figure 13, the humidity in Room 1 indicated little change over time, whereas that in Room 2 indicated almost no change.
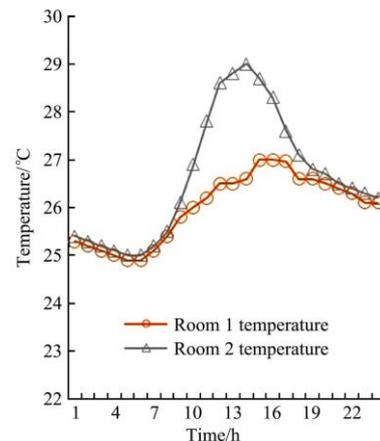
Figure 12   Temperature changes in the two rooms
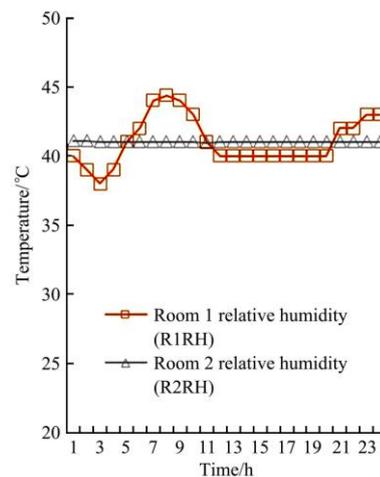
Figure 13   Relative humidity change

The highest and lowest recorded humidity levels in Rooms 1 and 2 were 44.4% and 43%, and 38% and 41%, respectively, whereas the average humidity levels were 41% and 42%, respectively.   The average humidity difference in the two rooms was only 1%.   It was concluded that the difference in the relative humidity was due to the coolness of the ground heat exchanger inside, which initially decreased the humidity, thus causing a much lower sensible temperature in Room 1 than that in Room 2.

4.3   Effects of the buried PE pipe material on ground heat exchange

Regarding the effects of the buried PE pipe material on the ground heat-exchanging performance, the pipe material does not have a significant impact on the heat-exchange efficiency according to the experimental study conducted by Kim et al.[32] Additionally, in a ground heat-exchanger performance analysis conducted by Go et al.[33], the effect on heat exchange from changing the pipe materials to PVC, PE, or steel was only 1.1%-2.1%, which was very minimal.   According to the experimental results, the heat conductivity of the actual soil was only 0.2-1.1 W/(m·℃), which was not large, and the heat-resisting effects during the heat transfer were minimal.   Thus, it was concluded that the material should be strong enough to satisfy the requirement for withstanding the soil pressure.

4.4   Cooling load

As seen in Figure 12, there was almost no time period for a resident to feel very hot.   Considering the indoor cooling design

temperature at 28 ℃, the maximum cooling load of the experimental building calculated according to Equations (5)-(8) was 2206 kJ/h.

5 Conclusions

The application of the ground cooling system for cooling rural houses in northeastern China was studied, and the conditions for the ground cooling system were proposed. The following conclusions can be drawn.

(1) Considering the indoor cooling design temperature at 28 ℃, the maximum cooling load was calculated 2206 kJ/h.

(2) According to the temperature change analysis per ground depth, a depth of 1.5-2 m should be adequate considering the workability, efficiency and frost line in northeastern China.

(3) The average temperature of the test room (Room 1) where the ground cooling system was installed was 3 ℃ lower than that of the control room (Room 2), and the effectiveness of the application of the ground cooling system was proven.

Nomenclature

Term	Unit	Description
H	kJ	Heat flux
Ke	kJ/(h·m·℃)	Effective thermal conductivity
$n\rho wCw$		Total amount of underground water (fluid) stored per unit volume of the underground medium
V		Velocity vector of underground water
T	℃	Temperature
Q_s	kJ/h	Solar heat acquired through the window
Q_c	kJ/h	Heat obtained through the surface of the building
Q_i	kJ/h	Sensible heat acquired by the infiltrated wind to the building
Q_{oa}	kJ/h	Heat generated by the human body indoors
Q_w	kJ/h	Latent heat
U	kJ/(h·m²·℃)	Total heat transfer coefficient
A	m²	Total surface area
V_i	m³/h	Air permeability
W_i	%	Relative humidity of indoor air
W_o	%	Relative humidity of outdoor air
ρ_w	kg/m³	water density
Subscript		
e		Effectivity
w		Water
x, y and z		Three-dimensional directions
i		Indoor
o		Outdoor
Abbreviations		
ACCA		Air-conditioning contractor of America
DETD		Design equivalent temperature difference

Acknowledgments

[References]

[1] Alev Ü, Eskola L. Renovation alternatives to improve energy performance of historic rural houses in the Baltic Sea region. Energy and Buildings, 2014; 77: 58–66.

[2] Hossein J, Seyed S M A, Rosen M A, Pourfallah M. Perfoumance of ground heat exchanger: A comprehensive review of recent advances. Energy, 2019; 178: 207–233.

[3] Mu X Z, Yu S S, Xu P. Review on utilizing rural biomass as energy. Modern Chemical Industry, 2018; 3: 9–13.

[4] Jang M K. Development and thermal performance of a solar thermal conversion system with vacuum tube solar collector and pebble bed storage. PhD dissertation, Shenyang Agricultural University, Shenayng, 2006; pp.8–16.

[5] Yim H J, Gong H J, Song Y S. Operating characteristics of opened ground thermal heat pump system. Transactions of Korean Society of the Equipment Engineering, 2004; 23(4): 701–706.

[6] Jang M K. Characteristics of heat storage and release of gravel layer in solar collectors by hot air natural circulation. Transactions of the CSAE, 2004; 21(8): 126–131. (in Chinese)

[7] Kim M J. A Study on the thermal characteristics of Jeju type ground heat exchanger for ground source pump system applied to Jeju Island. Journal of Korean Academia-Industrial cooperation Society, 2020; 21(2): 32–38.

[8] Bae Y. Performance analysis of geothermal exchanger in summer time. Dissertation for Doctorate of Kyungshang National University, Changweon, 2017; 22–27. (in Korean)

[9] Gong Y J, Zhang Y, Ning X F. Numerical simulation of cold storage and preservation of Hanfu apple. Journal of Biosystems Engineering, 2016; 41: 184–192.

[10] Badescu V, Sicre B. Renewable energy for passive house heating. Energy and Buidings, 2005; 35: 1077–1084.

[11] Zhai X Q, Dai Y J, Wang R Z. Experimental investigation on air heating and natural ventilation of a solar air collector. Energy and Buildings, 2015; 37: 373–381.

[12] Jiyong Y. Life cycle cost analysis of active solar house. Transactions of the Korean Society of Solar Energy, 2013; 12: 38–49.

[13] Hoon K, Geun J Y, Jae H P, Chang H L. Numerical study on heat transfer characteristics in branch tube type ground heat exchanger. Renewable Energy, 2018; 115: 585–599.

[14] Puri V M. Earth-tube heat exchanger performance correlation using boundary element method. Trans of the ASABE, 2007; 30(2): 514–520.

[15] Gao J J, Li, A B, Yan T. Ground heat exchangers: Applications, technology integration and potentials for zero energy buildings. Renewable Energy, 2018; 128: 337–349.

[16] Lekhal M C, Belarbi R, Mokhtari A M, Benzaama M H, Benna C R R. Thermal performance of a residential house equipped with a direct solar floor and an earth air heat exchanger. Sustainable Cities and Society, 2018; 40: 534–545.

[17] Javadi H, Ajarostaghi S S M, Zaboli M. Performance analysis of helical ground heat exchangers with different configurations. Applied Thermal Engineering, 2019; 154: 24–36.

[18] Kim M J, Yoon S, Lee S R, Kim W J, Go G H, Jeon J S. Evaluation of heat exchange rate in horizontal slinky and coil type ground heat exchangers considering pitch interval. Journal of the Korean Geotechnical Society, 2014; 30(7): 55–61. (in Korean)

[19] Park J I, Park K S. Analysis of earth design parameter and geothermal heat exchanger length in geothermal system. Journal of the Korean Society of Geothermal Energy Engineers, 2015; 11(3): 1–6.

[20] Leski K, Luty P, Larwa B. Numerical analysis of minimum ground temperature for heat extraction in horizontal ground heat exchangers. Energies, 2021; 14(17): 5487.

[21] Jeon J S, Lee S R, Kim M J, Yoon S. Suggestion of a scale factor to design spiral-coil-type horizontal ground heat exchangers. Energies, 2018; 11(10): 2736. doi: 10.3390/en11102736.

[22] Han J S. Geothermal pumping cooling & heating systems. Hanlim Publisher, 2011; 69–77. (in Korean)

[23] Par Y J, Kim K H. A study on the horizontal ground source heat pump greenhouse heating system with thermal storage tank. Journal of Energy Engineering, 2006; 15(3): 194–201.

[24] Seama K F, Rosen M A. Modeling of vertical ground heat exchangers. International Journal of Green Energy, 2020; 18(7): 755–774.

[25] Baek S H. Equivalent Thermal Model for ground heat exchangers considering ground temperature recovery. Transactions of Korean Institute of Architectural Sustainable Environment and Building Systems, 2020; 14(2): 147–157.

[26] Zhang T L, Wang L D. Design on cooling cycle system in rural areas. Journal of Chinese Agricultural Mechanization, 2016; 37(4): 237–241. (in China)

[27] Oh J. Introduction to solar heating, cooling & hot water systems: Concepts, design methods & economic analysis II. Yale Publishing, 2005; pp.130–135.

[28] Kwon Y K, Jae M K, Nam Y.   Study on the performance factor of the modular ground heat exchanger using CFD simulation.   Korean Journal of Air-Conditioning and Refrigeration Engineering, 2020; 32(7): 334–339.

[29] Puri V M. Feasibility and performance curves for intermittent earth-tube heat exchanger. Trans. of the ASABE, 2006; 29(2): 525–532.

[30] Pei W, Zhang M, Lai Y, Yan Z L.   Evaluation of the ground heat control capacity of a novel air-L-shaped TPCT-ground (ALTG) cooling system in cold regions.   Energy, 2019; 179: 655–668.

[31] Gan G H.   Dynamic thermal simulations of horizontal ground heat exchangers for renewable heating and ventilation of buildings. Renewable Energy, 2017; 103: 361–371.

[32] Kim Y B. Performance analysis of earth heat exchanger. Transactions of the Korean Society of Agricultural Machinery Solar Energy, 2016; 21(4): 436–448.

[33] Go C.   Heating effects & the operating problems of geothermal exchanger methods.   Journal of Agricultural Facilities, 2017; 12: 41–47.